C. Stan, S. Rommel, I. De Miguel, J. J. V. Olmos, R. J. Durán and I. T. Monroy, "5G Radio Resource Allocation for Communication and Computation Offloading," *2023 Joint European Conference on Networks and Communications & 6G Summit (EuCNC/6G Summit)*, Gothenburg, Sweden, 2023, pp. 1-6, https://doi.org/10.1109/EuCNC/6GSummit58263.2023.10188281

5G Radio Resource Allocation for Communication and Computation Offloading

Catalina Stan*, Simon Rommel*, Ignacio de Miguel†, Juan José Vegas Olmos‡, Ramón J. Durán†, Idelfonso Tafur Monroy*

*Department of Electrical Engineering, Eindhoven University of Technology, Eindhoven, The Netherlands

†Department of Signal Theory, Communications and Telematics Engineering, Universidad de Valladolid, Valladolid, Spain

‡NVIDIA Corporation, Ofer Industrial Park, Yokneam, Israel

{c.i.stan, s.rommel, i.tafur.monroy}@tue.nl, {ignacio.miguel, ramon.duran}@tel.uva.es, juanj@nvidia.com

***Abstract*—Edge computing is envisioned as a key enabler in future cellular networks by bringing the computing, networking and storage resources closer to the end users and enabling offloading for computation-intensive or latency-critical tasks coming from the emerging 5G/6G applications. Such technology also introduces additional challenges when it comes to deciding when to offload or not since the dynamic wireless environment plays a significant role in the overall communication and computation costs when offloading workload to the nearby edge nodes. In this paper, we focus on the communication cost in computation offloading via wireless channels, by formulating an α-fair utility-based radio resource allocation (RRA) problem tailored for offloading in a multi-user urban scenario where the uplink connection is the main focus. We begin by modeling the wireless channel with large- and small-scale fading at both lower and millimetre-wave frequencies, followed by data rate calculation based on 3GPP for a more realistic approach. Then, while assessing the fairness of the RRA, we simulate the resource allocation framework while taking into account both users who need to offload and users who are only interested in high downlink data rates. Simulation results show that the weighted proportional fairness method adapted for computation offloading can provide a good trade-off between fairness and performance compared to other benchmark schemes.**

***Keywords*—5G, edge computing, computation offloading, resource allocation, fairness**

I. Introduction

With demands fuelled by the emerging use cases and the continuous increase of connected devices, edge computing aims to extend the computing, storage and networking capabilities of cloud servers to the edge of the network [1]. As the long-distance data transmission from end devices to the cloud incurs great propagation delay, bringing the computational resources closer to mobile end users [2] reduces latency and allows applications to leverage the benefits of computation offloading since compute-intensive and latency-critical tasks are migrated to resourceful edge nodes. The inclusion of edge computing in standardization commonly follows the framework of multi-access edge computing (MEC) [3].

Although edge computing brings dynamicity into the network by allowing faster processing, the computing and storage resources of MEC hosts are limited compared to cloud data centers, and their availability is limited by the dynamic radio access network (RAN) domain where time-varying link states are highly influencing the communication quality between MEC hosts and end users. These aspects are especially important in scenarios where users are running computation-intensive applications such as augmented reality (AR), virtual reality (VR), face recognition or interactive gaming, to name but a few. In such cases, there is need for optimal decision-making where a decision can represent offloading all tasks to MEC (full offloading), processing on device (local execution), partial offloading, i.e., part of the tasks are executed on the user device while the rest is offloaded, and cloud execution possibly coming at the expense of reduced quality of experience (QoE). As offloading every computation task is not feasible, smart offloading decisions must be made by evaluating the overall offloading cost coming from the network and spectrum resources together with the energy consumption required to communicate and compute tasks using edge nodes [4]. This work focuses on the communication aspect of computation offloading where user equipment (UE) sends data packets to MEC for processing and expects the computation result on the downlink (DL). In an offloading scenario, data size (e.g. input parameters, program codes) transmitted on the uplink (UL) is often higher than the result transmitted on the DL [5], [6], therefore investigating radio resource allocation (RRA) techniques with emphasis on UL communication is essential when trying to make optimal offloading decisions. Furthermore, in multi-user wireless systems where different QoE has to be met for each user, the resource allocation problem takes on a new perspective where the trade-off between maximizing the overall system performance and ensuring fairness must be approached, taking into account that maximizing fairness may not be the best answer. In other words, users with poor signal-to-interference-plus-noise ratio (SINR) will experience resource starvation if the goal is to maximize the overall system performance since the resources will be distributed to users with better channel state. If the goal is to achieve high system fairness, users with unfavorable channel conditions benefit from more resources, but this comes at the cost of degrading the overall performance, therefore a balanced trade-off needs to be found [7].

Due to the always-changing wireless domain and the limited and expensive frequency spectrum, the efficient radio resource allocation has been a challenging issue over the years, especially in multi-user scenarios. Joint UL and DL resource allocation optimization problem was investigated with the objective to maximize system throughput [8]. The trade-off between resource efficiency and user fairness is studied in [9], where two adaptive resource allocation frameworks based on utility theory were proposed, suitable for real-time and non-real-time services. With recent advancements in artificial intelligence, reinforcement learning (RL) was employed

for networks with dynamic environments and dynamic user demands to tackle resource allocation problems where the trade-off between spectral efficiency and energy efficiency [10] or the optimization of both overall and fairness throughput [11] were investigated. In respect to computation offloading scenarios, various researches have been carried out for different types of networks, focusing on areas such as task partitioning, types of offloading decisions or minimization of energy consumption where one of the main aspects was to investigate resource allocation [4], [12]. Moreover, in offloading-related resource allocation discussions, data rate calculation is often based on the Shannon–Hartley theorem, while more realistic data rates are rather different. A joint optimization problem for offloading decisions and computational resource allocation was proposed in [13] where deep reinforcement learning (DRL) was employed to find the optimal solution. Similarly, DRL was employed to maximize the vehicular edge computing network utility by determining the offloading and resource allocation policies [14] or minimizing the total delay and resource usage in a joint offloading, resource allocation and service caching placement problem [5].

In this work, we focus on fair resource allocation for the communication aspect of computation offloading in a multi-user urban scenario. We first look at the channel models for urban macro (UMa) and urban micro (UMi) environments where we simulate statistical large- and small-scale fading conditions for both line-of-sight (LOS) and non-line-of-sight (NLOS) propagation. We continue with the calculation of more practical data rates based on 3GPP by looking at SINR and channel quality indicator (CQI) mapping in both frequency range (FR) 1 and 2 in order to contrast it with the Shannon capacity, which, to the best of our knowledge, it has not been approached in offloading studies. Then, we propose a fair RRA framework adapted for computation offloading where we weight the importance of UL and DL data rates and evaluate fairness. The objective function of the RRA problem is built on α-fair utility functions with constraints where higher α value indicates a higher degree of fairness. The weights of the proposed utility-based function can be adjusted to accommodate the needs of users that require offloading (higher UL data rate) and also for those who do not (higher DL data rate). We solve the optimization problem using disciplined convex programming and evaluate which functions are the most suitable in an offloading scenario based on the trade-off between overall performance and fairness.

The reminder of this paper is organized as follows. Section II introduces the system model together with channel modeling and data rate calculation. Section III describes the proposed RRA framework. Section IV provides a closer look at the simulation results. Section V concludes the paper and looks out to future developments.

II. System Model

In this section the system model is described together with channel modeling and data rate calculation. As shown in Figure 1, the system model is represented by the 5G RAN with one MEC host. The RAN domain is comprised of UMa cells using 3.5 GHz as carrier frequency, represented by the large hexagons, and UMi cells using 27.5 GHz as carrier frequency, represented by the small hexagons, distributed according to a frequency reuse factor of 1/3. The gNodeB is following a high and low layer functional split [15] of the radio stack and consists of multiple radio units (RUs) and distributed units (DUs) and one centralized unit (CU) co-located with the MEC host where data is offloaded for processing. During the simulation, we consider K serving RUs denoted by $\mathcal{K} = \{1, 2, ..., K\}$, each of them responding to the demands of I users denoted by $\mathcal{I} = \{1, 2, ..., I\}$. The user coordinates are generated based on a uniform distribution, while taking into account the inter-site distance (ISD) for both UMa and UMi. We also consider M neighbor RUs for DL interference denoted by $\mathcal{M} = \{1, 2, ..., M\}$ and N UEs for UL interference denoted by $\mathcal{N} = \{1, 2, ..., N\}$. The same numbers of network elements I, K, M and N are used for both UMa and UMi scenarios.

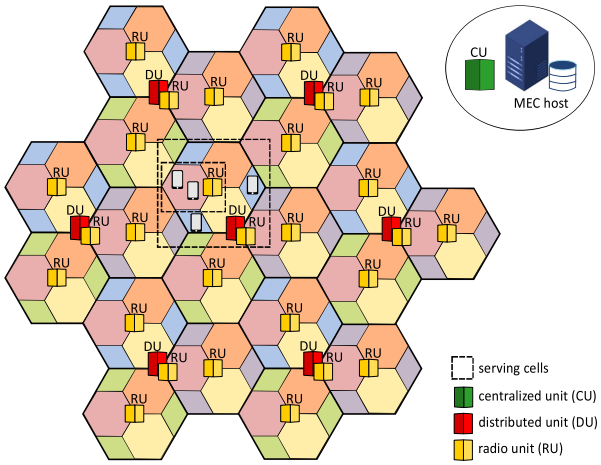

Fig. 1. System model comprised of UMa and UMi cells served by one gNodeB following the CU–DU–RU functional split and one MEC host.

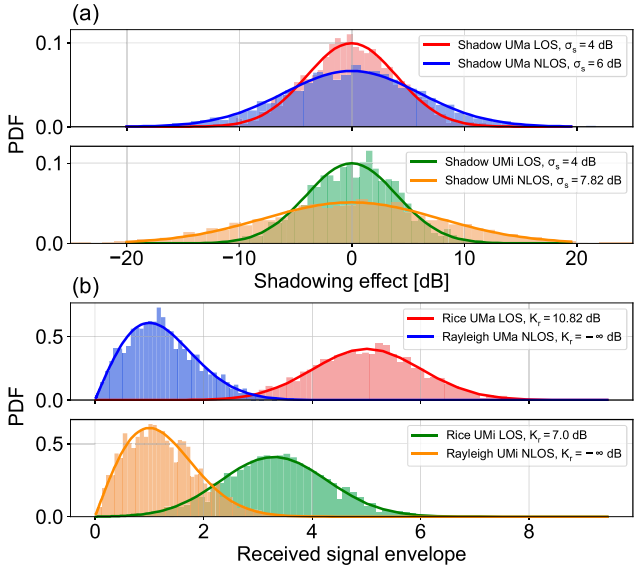

Fig. 2. Fading loss: (a) probability density function of shadowing loss for UMa and UMi in LOS and NLOS conditions, and (b) probability density function of Rice and Rayleigh distributions for small-scale fading.

A. Channel modeling

To understand the channel conditions that users in UMa and UMi scenarios may undergo, we simulated the 3GPP channel model [16] with large- and small-scale fading, considering both

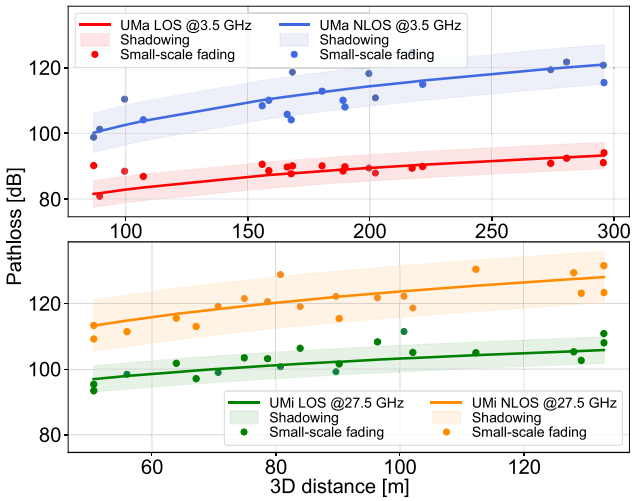

Fig. 3. Overall propagation loss for macro and micro cells under both LOS and NLOS conditions with large-scale fading – pathloss and shadowing shown as a range given by the standard deviation, and small-scale fading shown as specific samples when extracting random variates.

FR1 (0.41 GHz – 7.125 GHz) and FR2 (24.25 GHz – 52.6 GHz) frequencies. The model parameters are summarized in Table I. Figure 2 (a) shows the shadowing loss modeled as a Gaussian distribution on a logarithmic scale. The standard deviation σ_s does not change from FR1 to FR2 since the channel model is designed for frequencies under 100 GHz. Figure 2 (b) depicts the small-scale fading statistically modeled by the Rice distribution for LOS propagation where a dominant component is present, and Rayleigh distribution for NLOS propagation. Rice distribution is mainly characterized by the Rice factor K_r, representing the ratio between the power of LOS component, and average power of the sum of the NLOS components, where the NLOS components are denoted by σ_r^{NLOS}. In NLOS, K_r is equal to 0 (becoming a Rayleigh distribution), while for the LOS case, K_r is modeled as a Gaussian distribution with non-zero-mean μ_{K_r} and standard deviation σ_{K_r}. The overall propagation loss is calculated according to Eq. (1), where PL_0 is the calculated pathloss, S_{σ_s} is the shadowing loss and X_{σ_r} is the small-scale fading loss as follows

$$PL = PL_0 + S_{\sigma_s} + X_{\sigma_r}. \tag{1}$$

In Figure 3, large-scale fading (pathloss and shadowing) and small-scale fading are represented in both UMa and UMi scenarios for both LOS and NLOS. We can see that the fading loss increases with distance in both scenarios where the UMi NLOS case presents the highest propagation loss when moving to the millimetre-wave (mm-wave) frequency range. The distance is calculated as a 3D distance, where the 2D distance between the UE and RU as well as the UE and RU heights were taken into account. To evaluate the UE channel condition we looked at the DL SINR for user i served by RU k which can be expressed as follows

$$SINR_{k,i}^{\mathrm{DL}} = \frac{P_{\mathrm{RU}} G_{k,i}^{\mathrm{DL}}}{P_n + \sum_{m=1}^{M} P_{\mathrm{RU}} G_{m,i}^{\mathrm{DL}}}, \tag{2}$$

where P_{RU} represents the RU transmit power, different for UMa and UMi, $G_{k,i}^{\mathrm{DL}}$ is the DL channel gain from RU k to user i, where receiver antenna gain was also considered,

TABLE I. SIMULATION PARAMETERS

Parameter name	Unit	Value UMa	Value UMi
Carrier frequency f_c	GHz	3.5	27.5
Frequency reuse factor		1/3	1/3
Number of serving RUs K		1	1
Number of users I		20	20
Number of interfering RUs M		4	4
Number of interfering UEs N		6	6
ISD	m	500	250
Shadowing LOS σ_s	dB	4	4
Shadowing NLOS σ_s	dB	6	7.82
Rice K_r factor μ_{K_r}	dB	9	9
Rice K_r factor σ_{K_r}	dB	3.5	5
Small-scale fading σ_r^{NLOS}	Vrms	1	1
RU height	m	25	10
UE height	m	1.5	1.5
Effective environment height	m	1	1
Minimum 3D distance between UE and RU	m	35	10
Transmit power P_{RU}	dBm	53	47
Transmit power P_{UE}	dBm	20	23
Antenna gain RU	dB	20	20
Antenna gain UE	dB	3	3
NF RU	dB	1.5	3
NF UE	dB	4	4
Maximum bandwidth B	MHz	30	100
Number of component carriers J		1	1
Number of MIMO layers ν		1	1
Scaling factor f		1	1
Numerology μ		1	2
SINR lower limit	dB	−7	−7
UL weight w^{UL}		0.7	0.7
Maximum UL PRBs per user $n_{\mathrm{prb}_{\max}}^{\mathrm{UL}}$		17	9
Maximum DL PRBs per user $n_{\mathrm{prb}_{\max}}^{\mathrm{DL}}$		18	9
Maximum PRBs per channel $n_{\mathrm{prb}_{\max}}$		78	132

$P_n = k_B T_e B$ is the thermal noise power and $G_{m,i}^{\mathrm{DL}}$ is the DL channel gain of the interfering RU m to user i. Similarly, the UL SINR from user i to RU k is calculated as follows

$$SINR_{i,k}^{\mathrm{UL}} = \frac{P_{\mathrm{UE}} G_{i,k}^{\mathrm{UL}}}{P_n + \sum_{n=1}^{N} P_{\mathrm{UE}} G_{n,k}^{\mathrm{UL}}}, \tag{3}$$

where P_{UE} is the UE transmit power, different for UMa and UMi, and $G_{n,k}^{\mathrm{UL}}$ is the channel gain from the interfering user N to serving RU k. The final SINR values were obtained by subtracting the noise figure (NF) which has different values for UE and RU in FR1 and FR2.

B. Data rates

We explored two methods for data rate calculation since our proposed RRA framework described in Section III relies on data rate as output parameter. First, we start with the typical assumption of using the Shannon–Hartley theorem to obtain data rate r_i' for user i as

$$r_i' = B \log(1 + SINR_i), \tag{4}$$

where B is the channel bandwidth. Since we did not find this approach realistic enough, we moved toward more practical data rates calculated based on 3GPP [17], where data rate r_i for user i is defined as follows

$$r_i = \sum_{j=1}^{J} \left(\nu^{(j)} Q_m^{(j)} f^{(j)} R \frac{n_{\mathrm{prb}}^{BW_{(j),\mu}} 12}{T_s^{\mu}} (1 - OH^{(j)}) \right), \tag{5}$$

where J is the number of aggregated component carriers, ν is the number of multiple-input multiple-output (MIMO) layers, Q_m is the modulation order, f is the scaling factor, R is the code rate, $T_s^{\mu} = \frac{10^{-3}}{14 \cdot 2^{\mu}}$ is the average orthogonal frequency-division multiplexing (OFDM) symbol duration, μ is the 5G

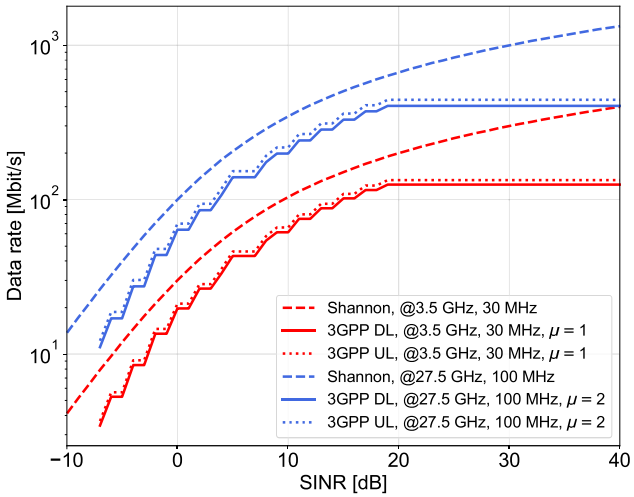

Fig. 4. Uplink and downlink data rate comparison between 3GPP and Shannon–Hartley as a result of SINR-CQI mapping.

NR numerology, n_{prb}^{BW} is the physical resource block (PRB) allocation for bandwidth BW with numerology μ and OH is the overhead.

To compare the two data rates, we mapped the SINR values to the corresponding channel quality indicators (CQI) using the linear expressions calculated in [18]. The CQI indices [19] take values between 0 and 15, where each value represents a pair of modulation scheme Q_m and code rate R. We selected $\mu = 1$ and 30 MHz bandwidth for UMa, and $\mu = 2$ and 100 MHz bandwidth for UMi. The comparison is displayed in Figure 4, where the data rate calculated with Eq. (5), having a staircase shape as a result of the SINR-CQI mapping, is significantly lower than the one calculated with Eq. (4) (the relative change compared to Shannon can be as least 30.1 % for DL data rates, excluding the flat region above 20 dB SINR, with an average relative difference of 42.32 % and 44.15 % for FR1 and FR2 respectively for common user SINR values between -7 and 30 dB). Moreover, we can observe that the UL data rate given in Eq. (5) is slightly higher compared to its DL counterpart, in both FR1 and FR2, due to differing overhead values [17]. In our simulation, we chose to exclude SINR values smaller than −7 dB in order to preserve the CQI values above 1. Given the above comparison, we select the number of PRBs n_{prb} as input for our RRA optimization problem and use the data rate calculation formula given in Eq. (5) since it provides values closer to what UEs will experience and allows giving more applicable guidance for actual network deployments.

III. Radio Resource Allocation for Offloading

This section describes the proposed RRA framework formulated as a joint UL and DL constrained optimization problem based on the weighted α-fair utility function. The resource that is being allocated is restricted to the frequency domain, more precisely each user i gets allocated an integer number of resource blocks $n_{\text{prb,i}}$. In addition, we adapt the problem to computation offloading where we allow different weights for UL and DL to represent the users' offloading preference.

Let the binary variable a_i denote the offloading preference of user i as follows

$$a_i = \begin{cases} 0, & \text{if UE } i \text{ is not offloading,} \\ 1, & \text{if UE } i \text{ is offloading.} \end{cases} \tag{6}$$

Then, the general α-fair utility function [20], $U_\alpha(r_i)$ in Eq. (7), is adapted as presented in Table II, where w_i^{UL} yields the weight attributed to UL data rate and α represents the fairness parameter where a higher α value means higher fairness in terms of resource allocation. The purpose of connecting w_i^{UL} and a_i in the proposed formulas is to allow weight flipping when offloading is needed or not, i.e., for users that do not wish to offload a higher weight is assigned to DL, while for users requiring offloading the higher weight is instead assigned to UL.

$$U_\alpha(r_i) = \begin{cases} w_i \log(r_i), & \text{if } \alpha = 1\ , \\ w_i \frac{r_i^{1-\alpha}}{1-\alpha}, & \text{otherwise.} \end{cases} \tag{7}$$

Given the proposed utility functions in Table II, we can summarize the scope of each utility as follows: the weighted maximum system efficiency with $\alpha = 0$ (referred to as Max SE) aims to maximize the overall system data rates without regard for fairness, the weighted proportional fairness with $\alpha = 1$ (referred to as PF) is an intermediate function with weak representation of fairness, while weighted harmonic mean fairness with $\alpha = 2$ (referred to as HMF) imposes the strongest fairness criteria out of the three, thus benefiting users with bad channel conditions, but at the cost of lower overall system performance. System fairness can be evaluated using Jain's fairness index [21] F defined as

$$F = \frac{(\sum_{i=1}^{I} r_i)^2}{I \sum_{i=1}^{I} r_i^2}. \tag{8}$$

To determine the possible trade-offs between fairness and overall system data rates, the RRA problem can be formulated as

$$\underset{r_i^{\text{UL}}, r_i^{\text{DL}}}{\text{maximize}} \quad \sum_{i=1}^{I} U_\alpha(r_i^{\text{UL}}, r_i^{\text{DL}}) \tag{9a}$$

$$\text{subject to}$$

$$n_{\text{prb},i}^{\text{UL}} \geq 1 \qquad \forall i, \tag{9b}$$

$$n_{\text{prb},i}^{\text{DL}} \geq 1 \qquad \forall i, \tag{9c}$$

$$n_{\text{prb},i}^{\text{UL}} \leq n_{\text{prb}_{\max}}^{\text{UL}} \qquad \forall i, \tag{9d}$$

$$n_{\text{prb},i}^{\text{DL}} \leq n_{\text{prb}_{\max}}^{\text{DL}} \qquad \forall i, \tag{9e}$$

$$\sum_{i=1}^{I} (n_{\text{prb},i}^{\text{UL}} + n_{\text{prb},i}^{\text{DL}}) \leq n_{\text{prb}_{\max}} \ \forall i, \tag{9f}$$

where constraints (9b) and (9c) guarantee at least one PRB per user for DL and UL, (9d) and (9e) limit the maximum number of PRBs that can be assigned for one user on UL and DL respectively, and (9f) indicates that the sum of all PRBs cannot be larger than the maximum available PRBs for the given bandwidth of the wireless channel. With objective (9a), we seek to maximize each utility function where the input is represented by the number of PRBs restricted to integer values. The solution is obtained using disciplined convex programming (DCP) and it will be described in Section IV. In addition to the three evaluated utility functions, equal PRB allocation for all users is further included in the evaluation to contrast between output (i.e., data rate) and input (i.e., PRB allocation) fairness. Since equal PRB allocation can result in unused spectrum, we further distribute the remaining PRBs randomly in order to cover the maximum available resources.

TABLE II. ADAPTED α-FAIR UTILITY FUNCTIONS

	α value	Utility function
Max SE	0	$U_\alpha(r_i^{\mathrm{UL}}, r_i^{\mathrm{DL}}) = (-1)^{a_i}((1-a_i) - w_i^{\mathrm{UL}})r_i^{\mathrm{UL}} + (-1)^{a_i+1}(a_i - w_i^{\mathrm{UL}})r_i^{\mathrm{DL}}$
PF	1	$U_\alpha(r_i^{\mathrm{UL}}, r_i^{\mathrm{DL}}) = (-1)^{a_i}((1-a_i) - w_i^{\mathrm{UL}})\log(r_i^{\mathrm{UL}}) + (-1)^{a_i+1}(a_i - w_i^{\mathrm{UL}})\log(r_i^{\mathrm{DL}})$
HMF	2	$U_\alpha(r_i^{\mathrm{UL}}, r_i^{\mathrm{DL}}) = (-1)^{a_i}((1-a_i) - w_i^{\mathrm{UL}})(-\frac{1}{r_i^{\mathrm{UL}}}) + (-1)^{a_i+1}(a_i - w_i^{\mathrm{UL}})(-\frac{1}{r_i^{\mathrm{DL}}})$

IV. SIMULATION RESULTS AND DISCUSSION

In this section we present the simulation results for the communication cost in a computation offloading scenario based on the proposed system model and the RRA scheme described in Sections II and III. In the simulation, we consider one UMa and one UMi cell, each cell serving 20 static users. For each user, we compute the channel conditions, i.e., large- and small-scale fading, followed by the UL and DL SINR calculation where all the interfering network elements (RUs or UEs) are considered to have NLOS propagation. Then, we randomly attribute one propagation type (LOS or NLOS) for each user and select only users with an acceptable SINR value, i.e., above −7 dB, as described in Section II. The offloading preference a_i is randomly distributed for each user i, and, for simplicity, we set the UL weight value w^{UL} to 0.7 for offloading users, which means that in a non-offloading scenario, the DL weight is also equal to 0.7. We calculated the maximum number of PRBs allowed for one user, $n^{\mathrm{UL}}_{\mathrm{prb_{max}}}$ and $n^{\mathrm{DL}}_{\mathrm{prb_{max}}}$, by selecting a relevant 5G quality of service identifier (5QI) for offloading, i.e., 5QI 90 which can be appropriate for mixed reality offloading applications [22]. As a result, $n^{\mathrm{UL}}_{\mathrm{prb_{max}}}$ and $n^{\mathrm{DL}}_{\mathrm{prb_{max}}}$ for UMa are equal to 17 and 18 PRBs respectively, while for UMi scenario, both $n^{\mathrm{UL}}_{\mathrm{prb_{max}}}$ and $n^{\mathrm{DL}}_{\mathrm{prb_{max}}}$ are equal to 9. The maximum channel capacity $n_{\mathrm{prb_{max}}}$ for UMa scenario operating at 3.5 GHz with a maximum bandwidth of 30 MHz is 78 PRBs [23], while for UMi operating at 27.5 GHz with a maximum bandwidth of 100 MHz is 132 PRBs [24]. The evaluation of the proposed utility functions is made based on 100 independent simulation runs, i.e., new channel conditions, propagation type and offloading preferences for each user. The list of parameters considered for the simulation is summarized in Table I.

To observe the simulation results, we first looked at Jain's fairness index calculated for UMa as illustrated in Figure 5 (a), where we can observe that the lowest fairness values are attributed to Max SE ($\alpha = 0$), while the highest values are obtained with HMF ($\alpha = 2$), the average fairness index value increasing by approximately three times. Similarly, the lowest fairness values in UMi come from Max SE, but the gap between Max SE and HMF is narrowed due to the larger maximum number of PRBs that can be assigned in FR2. In both UMa and UMi, the fairness index was calculated according to Eq. (8), where r_i is the weighted sum of DL and UL data rates. Based on the results in Table III, it is interesting to compare weighted PF and Equal PRB since both have similar fairness statistics and average UL and DL data rate sum per iteration.

Looking closer at the difference between the two methods, we find that the average UL data rate sum per iteration for UMa users in offloading scenario obtained with PF is 37 % higher compared to Equal PRB, as shown in Figure 6 (a), while the average DL data rate sum per iteration for users in non-offloading scenario is 36.86 % higher, as shown in Figure 6 (b), therefore confirming the influence of weights on the PRB assignment. Similar differences are found for UMi environment. Based on these results, weighted PF can offer a good trade-off between fairness and performance for users in offloading and non-offloading scenarios for both UMa and UMi. Therefore, users running compute-intensive applications with need to offload are assigned more PRBs for UL, translating into higher UL data rates, with 56.06 % increase compared to average DL data rate sum per iteration in the same scenario. For users with no need for offloading, the average DL data rate sum per iteration is 52.62 % higher compared to UL. Since the channel state is changing with each

TABLE III. FAIRNESS AND AVERAGE SUM DATA RATES

	UMa			UMi		
	Fairness		Avg. Σ data rate [Mbit/s]	Fairness		Avg. Σ data rate [Mbit/s]
	Mean	Std.		Mean	Std.	
Max SE	0.273	0.019	116.91	0.703	0.077	370.14
PF	0.835	0.060	96.65	0.840	0.062	307.87
HMF	0.913	0.041	76.30	0.918	0.041	255.13
Equal PRB	0.793	0.081	96.81	0.820	0.065	309.32

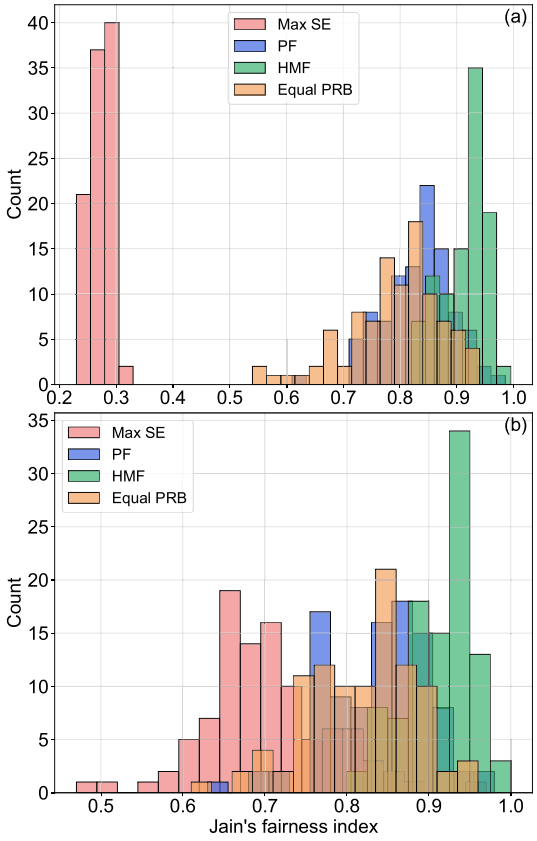

Fig. 5. Jain's fairness index for the proposed resource allocation in (a) UMa and (b) UMi scenarios.

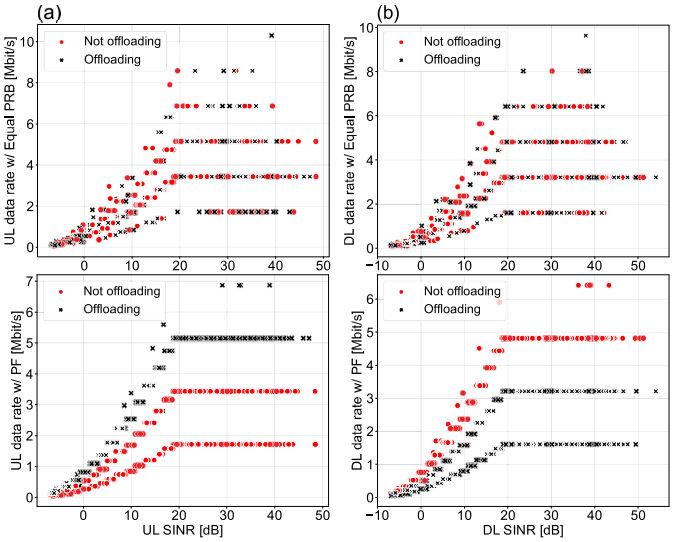

Fig. 6. Data rate variation in UMa representing the offloading preference: (a) with Equal PRB and weighted PF after UL PRB allocation, and (b) with Equal PRB and weighted PF after DL PRB allocation.

iteration, the number of users with SINR higher than -7 dB is also changing, therefore the number of PRBs allocated for DL and UL with weighted PF is varying between one and four PRBs in UMa scenario, as depicted in Figure 6 by the four data rate curves.

V. Conclusion

In this work we looked at 5G channel modeling for urban scenarios and calculated data rates using two methods – Shannon–Hartley and 3GPP, concluding that 3GPP can provide more realistic data rates, with difference as low as 30.1 % for DL data rates. Then, we proposed different weighted α-fair utility functions for resource allocation to accommodate the user needs in offloading and non-offloading scenarios where the weights varied according to the offloading preference. Considering the outcome of this work, we could see that weighted PF can achieve a good fairness-performance trade-off, outperforming Equal PRB allocation in terms of average UL data rate sum per iteration for offloading users with an increase of 37 %, and a similar increase in DL data rate for non-offloading users in UMa scenario. In future work, we will look out for additional parameters for more accurate channel modeling, moving toward MIMO and carrier aggregation for higher data rates, and DRL-based resource allocation solutions for faster decision-making and scalability, using this work as comparison.

Acknowledgment

This work was supported by the EU H2020 MSCA ITN-ETN IoTalentum project (grant no. 953442) and also in part by Consejería de Educación de la Junta de Castilla y León and the European Regional Development Fund (Grant VA231P20).

References

[1] N. Hassan, K.-L. A. Yau, and C. Wu, "Edge Computing in 5G: A Review," *IEEE Access*, vol. 7, pp. 127 276–127 289, 2019.

[2] P. Du, A. Nakao, L. Zhong, and R. Onishi, "Intelligent Network Slicing With Edge Computing for Internet of Vehicles," *IEEE Access*, vol. 9, pp. 128 106–128 116, 2021.

[3] ETSI GS MEC 003, "Multi-access Edge Computing (MEC); Framework and Reference Architecture," March 2022, v3.1.1.

[4] P. Mach and Z. Becvar, "Mobile edge computing: A survey on architecture and computation offloading," *IEEE Commun. Surv. Tutor.*, vol. 19, no. 3, pp. 1628–1656, 2017.

[5] S. Yu, X. Chen, Z. Zhou, X. Gong, and D. Wu, "When deep reinforcement learning meets federated learning: Intelligent multitimescale resource management for multiaccess edge computing in 5g ultradense network," *IEEE Internet Things J.*, vol. 8, no. 4, pp. 2238–2251, 2021.

[6] C. Wang, C. Liang, F. R. Yu, Q. Chen, and L. Tang, "Computation offloading and resource allocation in wireless cellular networks with mobile edge computing," *IEEE Trans. Wirel. Commun.*, vol. 16, no. 8, pp. 4924–4938, 2017.

[7] H. SHI, R. V. Prasad, E. Onur, and I. Niemegeers, "Fairness in wireless networks:issues, measures and challenges," *IEEE Commun. Surv. Tutor.*, vol. 16, no. 1, pp. 5–24, 2014.

[8] Z. Lin and Y. Liu, "Joint uplink-downlink resource allocation in ofdma cloud radio access networks," in *2018 IEEE International Conference on Communications (ICC)*, 2018, pp. 1–6.

[9] E. B. Rodrigues and F. Casadevall, "Control of the trade-off between resource efficiency and user fairness in wireless networks using utility-based adaptive resource allocation," *IEEE Commun Mag*, vol. 49, no. 9, pp. 90–98, 2011.

[10] Z. Liu, X. Chen, Y. Chen, and Z. Li, "Deep reinforcement learning based dynamic resource allocation in 5g ultra-dense networks," in *2019 IEEE International Conference on Smart Internet of Things (SmartIoT)*, 2019, pp. 168–174.

[11] S. Yin and F. R. Yu, "Resource allocation and trajectory design in uav-aided cellular networks based on multiagent reinforcement learning," *IEEE Internet Things J.*, vol. 9, no. 4, pp. 2933–2943, 2022.

[12] C. Jiang, X. Cheng, H. Gao, X. Zhou, and J. Wan, "Toward computation offloading in edge computing: A survey," *IEEE Access*, vol. 7, pp. 131 543–131 558, 2019.

[13] J. Li, H. Gao, T. Lv, and Y. Lu, "Deep reinforcement learning based computation offloading and resource allocation for mec," in *2018 IEEE Wireless Communications and Networking Conference (WCNC)*, 2018, pp. 1–6.

[14] Y. Liu, H. Yu, S. Xie, and Y. Zhang, "Deep reinforcement learning for offloading and resource allocation in vehicle edge computing and networks," *IEEE Trans. Veh. Technol.*, vol. 68, no. 11, pp. 11 158–11 168, 2019.

[15] ITU-T GSTR-TN5G, "Transport network support of IMT-2020/5G," February 2018.

[16] 3GPP TR 38.901, "Study on channel model for frequencies from 0.5 to 100 GHz," March 2022, v17.0.0.

[17] 3GPP TS 38.306, "User equipment (UE) radio access capabilities," June 2022, v17.1.0.

[18] Y. Wang, W. Liu, and L. Fang, "Adaptive modulation and coding technology in 5g system," in *2020 International Wireless Communications and Mobile Computing (IWCMC)*, 2020, pp. 159–164.

[19] 3GPP TS 38.214, "Physical layer procedures for data," September 2022, v17.3.0.

[20] J. Mo and J. Walrand, "Fair end-to-end window-based congestion control," *IEEE/ACM Transactions on Networking*, vol. 8, no. 5, pp. 556–567, 2000.

[21] R. Jain, D. Chiu, and W. Hawe, "A quantitative measure of fairness and discrimination for resource allocation in shared computer systems," 1998. [Online]. Available: https://arxiv.org/abs/cs/9809099

[22] ITU-T GSTR-5GQoE, "Quality of experience (QoE) requirements for real-time multimedia services over 5G networks," June 2022.

[23] 3GPP TS 38.101-1, "User Equipment (UE) radio transmission and reception; Part 1: Range 1 Standalone," June 2022, v17.6.0.

[24] 3GPP TS 38.101-2, "User Equipment (UE) radio transmission and reception; Part 2: Range 2 Standalone," June 2022, v17.6.0.